Circadian Clock Parameter Measurement: Characterization of Clock Transcription Factors Using Surface Plasmon Resonance

John S. O'Neill, Gerben van Ooijen, Thierry Le Bihan and Andrew J. Millar

J Biol Rhythms 2011 26: 91

DOI: 10.1177/0748730410397465

Circadian Clock Parameter Measurement: Characterization of Clock Transcription Factors Using Surface Plasmon Resonance

John S. O'Neill,*,† Gerben van Ooijen,† Thierry Le Bihan,† and Andrew J. Millar[1,†]

*Department of Clinical Neurosciences, University of Cambridge Metabolic Research Laboratories, Institute of Metabolic Science, Addenbrooke's Hospital, Cambridge, UK, and †Centre for Systems Biology at Edinburgh, Edinburgh, UK

Abstract To refine mathematical models of the transcriptional/translational feedback loop in the clockwork of *Arabidopsis thaliana*, the investigators sought to determine the affinity of the transcription factors LHY, CCA1, and CHE for their cognate DNA target sequences in vitro. Steady-state dissociation constants were observed to lie in the low nanomolar range. Furthermore, the data suggest that the LHY/CCA1 heterodimer binds more tightly than either homodimer and that DNA binding of these complexes is temperature compensated. Finally, it was found that LHY binding to the evening element in vitro is enhanced by both molecular crowding effects and by casein kinase 2–mediated phosphorylation.

Key words *Arabidopsis*, evening element, temperature compensation, SPR, DNA binding, circadian transcription factor, LHY/CCA1, molecular crowding, CK2

In *Arabidopsis thaliana*, models of cellular circadian rhythms have focused primarily upon transcriptional-translational feedback loops (TTFL), at the core of which lie several myb-family transcription factors, most notably LHY and CCA1 (Harmer, 2009), that contain a single DNA-binding myb-domain (Hofr et al., 2008). Overexpression of either LHY or CCA1 results in essentially arrhythmic plants, and in doubly null homozygous lines rhythmicity is also severely affected (McClung, 2006). The dawn-phased expression of these proteins is hypothesized to facilitate activation of morning-expressed downstream targets through binding to upstream cis-morning element (ME) promoter sequences, for example, the *PSEUDO-RESPONSE REGULATOR 9 (PRR9)* promoter, while repressing the transcription of dusk-phased genes bearing upstream evening element (EE) promoter sequences, for example, *CCR2* (Harmer and Kay, 2005; Locke et al., 2006). Promoter sequence determinants contribute to these alternative functions (Harmer and Kay, 2005), but the full extent of their contribution is unclear. Recent data have shown that LHY and CCA1 form functional homo- and heterodimers, both in vivo and in vitro (Lu et al., 2009; Yakir et al., 2009). CCA1 is also subject to functionally relevant posttranslational modification by casein kinase II (CK2) (Daniel et al., 2004; Yakir et al., 2009). While many other proteins have been strongly implicated in sustaining the molecular clockwork in plants (e.g., TOC1, PRR5/7/9, ELF3/4), their transcriptional targets remain less well characterized (McClung, 2006). Recently, however, a novel role was discovered for the transcription factor TCP21/CHE in facilitating the nighttime repression of CCA1 (Pruneda-Paz et al., 2009).

1. To whom all correspondence should be addressed: Andrew J. Millar, University of Edinburgh, C.H. Waddington Building, King's Buildings, Mayfield Road, Edinburgh EH9 3JD UK; e-mail: Andrew.Millar@ed.ac.uk.

JOURNAL OF BIOLOGICAL RHYTHMS, Vol. 26 No. 2, April 2011 91-98
DOI: 10.1177/0748730410397465

Of late, detailed mathematical models of this TTFL in the *Arabidopsis* clock have been extremely successful in describing and predicting qualitative and quantitative features of rhythmic gene expression (Edwards et al., 2010; Locke et al., 2006; Pokhilko et al., 2010). Such models reproduce 2 key features of circadian rhythms, namely entrainment and the free-running period (under constant conditions) (Pittendrigh, 1960), and have been tested for relevance to the control of period by temperature (temperature compensation) (Gould et al., 2006). Due to the paucity of quantitative biochemical data, however, by necessity parameter values for these models have largely been derived by fitting to time series data of transcript and protein accumulation or from bioluminescent reporters for these components, almost all at the "laboratory standard" temperature, 22 °C (Locke et al., 2005; Pokhilko et al., 2010; Zeilinger et al., 2006). Thus, the biological relevance of any given model's optimal parameter set to rhythms in vivo remains poorly explored. To further constrain our mathematical model of the *Arabidopsis* clockwork, we are engaged in the systematic quantification of key mechanistic parameters.

In the first instance, we have characterized the affinity of previously identified clock-relevant transcription factors for their cognate promoter motifs. To accomplish this we have employed surface plasmon resonance (SPR), a robust biophysical technique ideally suited to analysis of protein-DNA interactions (Majka and Speck, 2007). Briefly, protein is flowed over a streptavidin chip surface to which DNA duplexes have been immobilized. Biomolecular interactions are detected in real time through monitoring the change in refractive index of polarized light that is totally internally reflected on the reverse side of the chip. Once the reaction reaches an equilibrium, the binding affinity of the protein-DNA complex can be described as

$$R_{eq} = [\text{Protein}] \cdot R_{max} / ([\text{Protein}] + K_d)$$

where R_{eq} and R_{max} are the equilibrium and maximal response, respectively; and K_d is the dissociation constant, an indicator of binding affinity. By using several protein concentrations, the K_d can be reliably estimated (Majka and Speck, 2007).

MATERIALS AND METHODS

Materials

SA chips and 10x HBS-EP$^+$ buffer were from Biacore (Piscataway, NJ). All other materials were purchased from Sigma-Aldrich (Poole, UK) unless otherwise stated.

Oligos

The following oligonucleotide (nt) sequences were purchased from Invitrogen (Renfrew, UK).

Morning/evening element–containing promoter sequences (Harmer and Kay, 2005):

Bi-wt*CCR2*_FOR: 5′-GAGGTCAAACCTAGAAAATATCTAAACCTTGAAACCTAG-3′
wt*CCR2*_REV: 5′-CTAGGTTTCAAGGTTTAGATATTTTCTAGGTTTGACCTC-3′
Bi-wt*PRR9*_FOR: 5′-CGATCACAACCACGAAAATATCTTCTCAGAGAAAGAAGA-3′
wt*PRR9*_REV: 5′-TCTTCTTTCTCTGAGAAGATATTTTCGTGGTTGTGATCG-3′
Bi-CBS_*PRR9*_FOR: 5′-CGATCACAACCACGAAAAAATCTTCTCAGAGAAAGAAGA-3′
CBS_*PRR9*_REV: 5′-TCTTCTTTCTCTGAGAAGATTTTTTCGTGGTTGTGATCG-3′

Morning/evening element control sequences (Harmer and Kay, 2005):

Bi-mut*CCR2*_FOR: 5′-GAGGTCAAACCTAGAAAATCGAGAAACCTTGAAACCTAG-3′
mut*CCR2*_REV: 5′-CTAGGTTTCAAGGTTTCTCGATTTTCTAGGTTTGACCTC-3′
Bi-mut*PRR9*_FOR: 5′-CGATCACAACCACGAAAATCGAGTCTCAGAGAAAGAAGA-3′
mut*PRR9*_REV: 5′-TCTTCTTTCTCTGAGACTCGATTTTCGTGGTTGTGATCG-3′

TCP-binding site-containing sequences (Pruneda-Paz et al., 2009):

Bi-w*tCCA1*_FOR: 5′-ACGATCTTAAGTAGGTCCCACTAGATCAAGATATTATAAC-3′
wt*CCA1*_REV: 5′-GTTATAATATCTTGATCTAGTGGGACCTACTTAAGATCGT-3′
TCP-binding site control sequences:
Bi-mut*CCA1*_FOR: 5′-ACGATCTTAAGTATTGAAACATAGATCAAGATATTATAAC-3′
mut*CCA1*_REV: 5′-GTTATAATATCTTGATCTATGTTTCAATACTTAAGATCGT-3′

Protein Purification

At*CCA1* (NM_180129) and At*LHY* (NM_001083968) were cloned into pMAL-c2x-His_6 to express fusion proteins encoding N-terminal MBP (maltose binding protein) and C-terminal His_6 tags with predicted molecular weights of 111 kDa and 115 kDa, respectively. All

constructs were expressed in Rosetta pLysS (Merck KGaA, Darmstadt, Germany) overnight at 16 °C using 300 μM IPTG. The following day, cell pellets were resuspended in column buffer (phosphate-buffered saline, 20 mM imidazol, 1/7500 β-mercaptoethanol, 0.1 mM AESBF) and flash frozen in liquid nitrogen. Briefly, fusion proteins were affinity purified sequentially using first Ni-NTA resin (Qiagen, Valencia, CA) and then amylose resin (NEB, Ipswich, MA), following the manufacturers' instructions. Following elution in HBS-EP$^+$ buffer (20 mM HEPES, 150 mM NaCl, 3 mM EDTA, 0.05% surfactant P20, 1 mM TCEP, pH 7.4) + 10 mM maltose, protein purity was assessed by Coomassie-stained SDS-PAGE (Supplemental Figure S1), and dialyzed overnight into HBS-EP$^+$ buffer at 4 °C. Protein concentration was estimated by OD_{280} and Bradford assay, prior to performing functional assays of active protein concentration using calibration-free concentration analysis (Persson, 2008), whereby the concentration of DNA-binding activity in solution was quantified. This value was typically 0.3 to 0.5 of that determined by OD_{280}. LHY/CCA1 was produced by mixing LHY and CCA1 in equimolar ratio immediately prior to experiments. While it would have been preferable to cleave the MBP tag off the transcription factor before performing these experiments, doing so was observed to lead to precipitation. As no detectable binding was found using MBP alone, and because the observed nanomolar affinity was consistent with that of other members of the protein family bearing multiple myb domains, we are satisfied that the determined values should be broadly indicative of those encountered in vivo. GST-CHE was kindly donated by Steve Kay (UC San Diego) and purified as described previously (Pruneda-Paz et al., 2009).

In Vitro Phosphorylation and Molecular Crowding

MBP-LHY-His_6 was dialyzed into CK2 buffer (20 mM Tris-HCl, 50 mM KCl, 10 mM $MgCl_2$, 1 mM TCEP, 200 μM GTP pH 7.5) and incubated with 1:2000 recombinant CK2 (NEB) at 30 °C, with shaking at 60 rpm, for 30 min before being dialyzed back into HBS-EP$^+$ buffer overnight at 4 °C.

Dextran (35–45 kDa, Sigma D1662) was dissolved to 5% or 10% (wt/vol) in HBS-EP$^+$.

Mass Spectrometry

Refer to supplementary online material, available at http://jbr.sagepub.com/supplemental.

Immobilization of Biotinylated DNA on the SA Sensor Chip.

All experiments were performed on a Biacore T100 (GE Healthcare, Chalfont St. Giles, UK), with immobilization of cognate and noncognate sequences on SA-chips. Briefly, 40-nucleotide, 5′-biotinylated single-stranded oligos from relevant Arabidopsis promoter sequences were bound to chip surfaces of flow cells (Fc) Fc2, Fc3, and Fc4 using injections at 5 μL/min. Fc1 was left blank and was used throughout for reference subtraction. DNA duplexes were formed by injecting complementary 40-nt single-stranded oligonucleotides into the appropriate Fc zone until saturation was observed. Total R_{ligand} bound was chosen such that R_{max} was 30 or less for any given protein-DNA interaction. Calibration-free concentration analysis (CFCA) was performed according to the manufacturer's instructions (Persson, 2008) using diffusion coefficients derived by assuming these proteins to be semi-elongated.

Surface Plasmon Resonance (SPR) Analysis

Purified protein was diluted serially in HBS-EP$^+$ buffer to yield several different concentrations typically ranging from 0.1 nM to 1000 nM. Varying concentrations were injected, in triplicate, across all Fc zones for 150 sec at 75 μL/min flow rate. Steady-state binding was always observed. Dissociation was then observed for 600 sec, prior to regeneration of the chip surface using injections of 0.1% SDS, 3 mM EDTA for 60 sec at 100 μL/min. Responses from the reference cell (Fc1) were subtracted to correct for nonspecific binding.

SPR Data Analysis

For reversible reactions between protein transcription factor (TF) and DNA:

$$TF + DNA \leftrightarrow TF{:}DNA, \text{ at equilibrium: } K_d = [TF{:}DNA]/[TF] + [DNA]$$

The equilibrium constant (K_d) may be determined from biosensor data once reactions reach a steady response during the association phase (Majka and Speck, 2007), and the observed binding responses of the transcription factors under study to their cognate DNA sequences fit this criterion. The response value at equilibrium was determined by averaging the reference-subtracted signal from 3 replicates after the start of each protein injection. For a fixed concentration of DNA ligand, these response values vary as a function of protein concentration and represent the

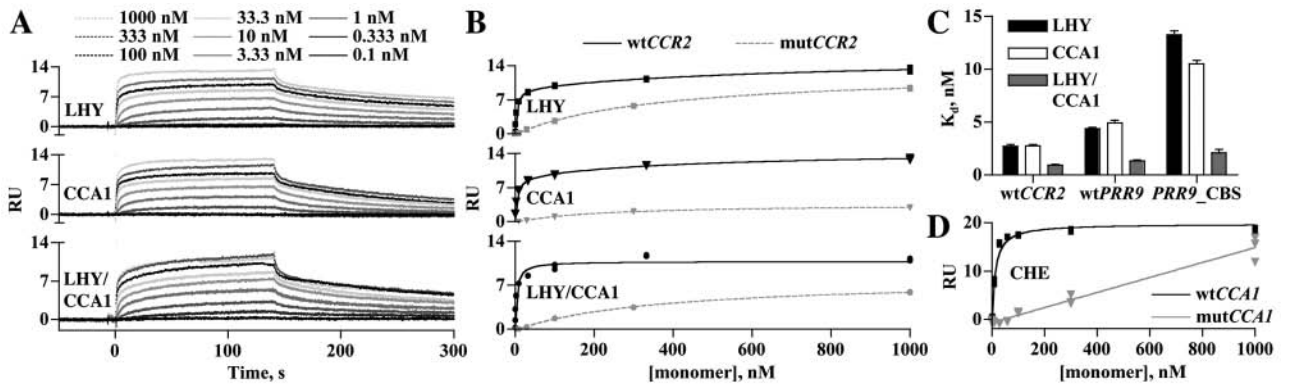

Figure 1. LHY and CCA1 bind synergistically to the evening element in vitro with nanomolar affinity at 12 °C. (A) Representative binding response curves for MBP-tagged LHY, CCA1, and an LHY/CCA1 mixture to a 40 nt double-stranded EE-containing sequence from the *CCR2* promoter (RU, response units). (B) Steady-state binding level (data points) and affinity fit (solid line) for protein binding to wt*CCR2* (black) and mut*CCR2* (grey). K_d^1 values (nM) were LHY, 3.94 ± 0.23; CCA1, 4.53 ± 0.47; LHY/CCA1, 1.44 ± 0.20. K_d^2 values were greater than 300 μM. (C) Grouped data for K_d^1 of MBP-tagged LHY, CCA1, and LHY/CCA1 binding to wild-type *CCR2* and *PRR9* and *PRR9*_CBS promoter sequences. Error bars indicate standard error, *n* = 3. (D) Steady-state binding level (data points) and affinity fit (solid line) for binding of GST-CHE to a 40 nt sequence from the wt*CCA1* (black) or mut*CCA1* (grey) promoter spanning the TCP-binding sequence.

amount of protein-DNA complex ($[TF:DNA]_{eq}$) formed at each protein concentration ([TF]). The equilibrium dissociation constant (K_d) can be determined from nonlinear least-squares curve fitting of the data to

$$[TF:DNA]_{eq} = TF:DNA_{max}(1/(1 + K_d/[TF]))$$

where $TF:DNA_{max}$ represents the maximum capacity of the surface in response units (RU).

BIAevaluation 2.0.1 software (GE Healthcare) was used to derive these binding parameters. Thus, binding at control and experimental results are taken into account to allow for quantitative steady-state affinity analysis. All fits presented exhibited chi-square less than 2. The steady-state equilibrium dissociation constant (K_d) was calculated assuming a 2-site affinity model, which fit appreciably better than a 1-site model, where

$$\text{Response} = ([TF] \cdot R_{max}^1)/([TF] + K_d^1) + ([TF] \cdot R_{max}^2)/([TF] + K_d^2).$$

The higher affinity (stronger) interaction (K_d^1) is reported in each case. Curves were exported and replotted in GraphPad Prism. Separate figures are the result of separate experiments. Significant bulk contributions/mass transport effects were not encountered throughout. Similar K_d estimates were obtained using kinetic analysis of the SPR data and, for several interactions, also using iso-thermal calorimetry (unpublished results) but were deemed less reliable.

DNA-protein complex stoichiometry was estimated using the following equation:

$$n = R_{max} \cdot (MW_{DNA}/(R_{DNA} \cdot MW_{TF}))$$

where n = the number of protein molecules bound to DNA, R_{max} = response for saturating concentration of protein, R_{DNA} = amount of immobilized DNA (RU), and MW_{DNA} and MW_{TF} = molecular weight of DNA and TF, respectively.

RESULTS

LHY and CCA1 Bind Synergistically to Morning and Evening Element Sequences with Nanomolar Affinity In Vitro

MBP-LHY-His_6 (LHY) and MBP-CCA1-His_6 (CCA1) of greater than 95% purity (Supplemental Figure 1) were serially diluted and used to assess binding to immobilized DNA duplexes. LHY and CCA1 have previously been shown to bind to evening element (EE) sequences as homodimers and heterodimers in vivo and in vitro (Lu et al., 2009; Yakir et al., 2009). In initial experiments using the wild-type EE-containing *CCR2* promoter sequence, we observed complex binding under steady-state conditions that was best fit using a 2-site model that yielded both a low (<30 nM, K_d^1) and a high dissociation constant (>300 nM, K_d^2). In contrast, binding to the mutated *CCR2* promoter

sequence was observed to be weak, failing to reach saturation at 1 μM total protein, and thus cannot be accurately quantified but was certainly greater than 300 nM. We therefore inferred that LHY and CCA1 have a weak non–sequence-specific affinity for double-stranded DNA in the low micromolar range but with a nanomolar affinity for their target sequences. The derived stoichiometry of binding was consistently between 1.6 and 1.9, implying a likely stoichiometry of 2:1 between protein and DNA duplex, as expected.

Under steady-state conditions at 12°C, the specific binding affinity (K_d^1) of LHY and CCA1 for morning/evening element–containing sequences from the *CCR2* and *PRR9* promoters was calculated to lie in the low nanomolar range (Figure 1, A-C). In contrast, binding of these transcription factors to noncognate sequences in which 4 bases from the evening element consensus had been altered (Harmer and Kay, 2005) showed much weaker affinity (>300 μM), highlighting the specificity for target sequences under these conditions (Figure 1A, 1B). This is consistent with previously published gel shift assays (Harmer and Kay, 2005). The affinity for EE is in the same order of magnitude as that reported for c-myb (containing 3 myb repeats) (Oda et al., 1999). No detectable binding was observed for MBP alone, following reference subtraction, within the concentration ranges assayed (not shown).

It has previously been reported that more than 90% of luminescent plants transformed with a synthetic *PRR9*-LUC construct behind multimerized EE sequences show rhythmic reporter expression (Harmer and Kay, 2005). However, rhythmicity was less frequent in plants transformed with a construct in which the EEs were replaced with CCA1 Binding Sites (CBS), a promoter element that is also present in the native *PRR9* promoter. Rhythms generated with either construct were evening-phased. Intriguingly, while the affinity of either LHY or CCA1 for *PRR9*_CBS is significantly weaker than for evening elements from either *CCR2* (evening) or *PRR9* (morning) ($p < 0.001$, t test, $n = 3$), the affinity of LHY/CCA1 for PRR_CBS is not significantly different than that for *PRR9* ($p > 0.1$, t test, $n = 3$) (Figure 1C). The lower affinity of the homodimers might contribute to the lower percentage of rhythmic plants conferred by the CBS_PRR9 construct (Harmer and Kay, 2005), but the similar affinity of the heterodimer for both elements calls that into question. Taking the results together, the lower affinity in vitro can only explain weakened rhythms if CCA1 or LHY bind the CBS element principally as homodimers. In vivo experiments are necessary to substantiate these assumptions.

We also analyzed the binding of the recently identified regulator of the *CCA1* promoter, CHE/TCP21, to its cognate T-box element in the *CCA1* promoter. Using recombinant GST-CHE, we observed a binding affinity in the low nanomolar range (9.4 ± 1.6 nM) compared with weak binding to a mutated sequence (>1 μM, Figure 1D). No binding was observed for GST alone over the same concentration ranges (not shown).

LHY and CCA1 Binding Is Temperature Compensated In Vitro

Temperature compensation is an important characteristic of a circadian system, but its molecular basis is unclear. To assess the temperature dependency of transcription factor binding to morning/evening elements, we assayed the steady-state binding affinity of the LHY or CCA1 homodimers and the LHY/CCA1 heterodimer over a range of biologically relevant temperatures. Surprisingly, K_d for all 3 ligands appeared to exhibit temperature compensation (Figure 2, A-C), with $Q_{10} < 1.3$ for binding to the 3 promoter sequences tested.

LHY Binding Affinity Is Increased by Molecular Crowding Effects In Vitro

Previous work has highlighted that the nuclear environment is densely populated and that the diffusive space available to macromolecules can be significantly lower than the nuclear volume might suggest (Richter et al., 2008). To re-create this molecular crowding phenomenon in vitro, we studied the binding of LHY to the evening element under conditions of increasing dextran concentrations. Dextran has been used as a proxy for cellular macromolecules in this context before (Mouillon et al., 2008). Consistent with expectations, we observed a greater than 2-fold increase in the steady-state affinity of LHY for its cognate *CCR2* and *PRR9* sequences in 5% and 10% dextran (Figure 3A, 2-way ANOVA, dextran effect, $p < 0.0001$, $n = 3$).

LHY Binding Affinity Is Increased by CK2-Mediated Phosphorylation In Vitro

Several studies have shown that LHY and CCA1 are subject to functionally relevant posttranslational modification by casein kinase II (CK2) (Daniel et al., 2004; Sugano et al., 1998; Sugano et al., 1999). To assess whether CK2-mediated phosphorylation of LHY had any functional effect on DNA binding, we phosphorylated LHY in vitro using recombinant CK2. Using a

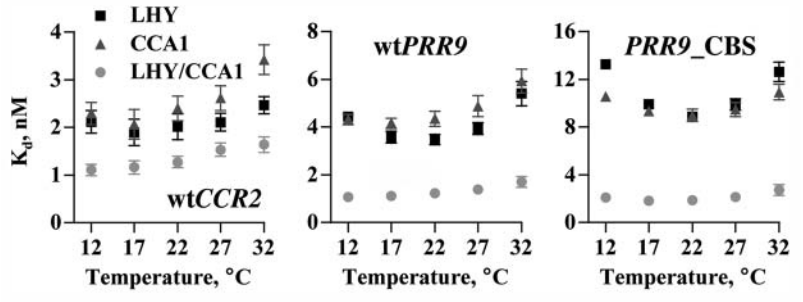

Figure 2. LHY and CCA1 binding is temperature compensated. Steady-state affinity of LHY, CCA1, and LHY/CCA1 binding to *CCR2*, *PRR9*, and *PRR9*_CBS promoter sequences over a range of biologically relevant temperatures.

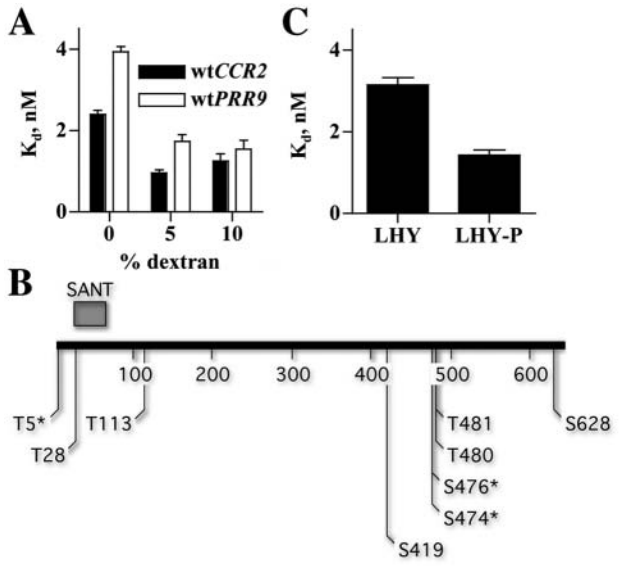

Figure 3. LHY binding affinity is affected by molecular crowding and phosphorylation. (A) Grouped data for K_d of MBP-tagged LHY binding to *CCR2* and *PRR9* promoter sequences in 5% or 10% dextran at 12 °C. (B) Phospho-mapping of in vitro phosphorylated LHY. *Conserved residues also phosphorylated in vivo in CCA1 homologue. (C) Grouped data for K_d of LHY and phosphorylated LHY (LHY-P) binding to the *CCR2* promoter at 12 °C.

TiO_2 phosphopeptide enrichment method followed by LC-MS analysis revealed 9 unique phospho-residues (Figure 3B), including 3 sites conserved in CCA1 that have previously been identified as being functionally relevant (Daniel et al., 2004) (Supplemental Figure S2). The other phospho-sites may or may not be relevant targets in vivo. A significantly stronger affinity of phosphorylated LHY (LHY-P) for the *CCR2* promoter was observed compared with unphosphorylated LHY (Figure 3C, unpaired *t* test, $p = 0.0015$, $n = 3$).

DISCUSSION

LHY and CCA1 are thought to play central, although semi-redundant roles in regulating the circadian clock in plants. Using real-time bioluminescent reporters in *Arabidopsis*, it has previously been shown that while they are expressed at different circadian phases, the *CCR2* and *PRR9* promoters are both regulated by a subset of the myb-family transcription factors, including LHY and CCA1, through their cognate morning/evening element sequences (McClung, 2006). Assuming *CCR2* and *PRR9* to contain promoter elements representative of the wider class observed in the upstream promoters of many clock-regulated genes, we sought to characterize the DNA binding of LHY and CCA1 transcription factors in vitro.

Single myb-domain proteins have previously been reported to form functional multimers when binding to DNA. We observed a binding interaction that is complex in nature, with an apparent stoichiometry of ~2:1, and to which a 2-site steady-state affinity model fit appreciably better than 1:1. In light of recent reports of functional homo/heterodimers of LHY and CCA1 in vitro and in vivo, it seems likely that these proteins exist as dimers in solution with a nonspecific weak affinity for relaxed double-stranded DNA (K_d^2) but with a much stronger, low nanomolar affinity for their cognate targets. The possibility of functional hetero- and homo-dimerization of LHY and CCA1 upon target sequences is supported here by the observation that LHY and CCA1 act synergistically to bind their target sequences in vitro as significantly greater binding is detected at a given concentration for an LHY/CCA1 mixture than for LHY or CCA1 alone. This is reflected by a more than 2-fold increase in steady-state affinity of LHY/CCA1, compared with LHY or CCA1, for wild-type *CCR2* and *PRR9* evening/morning element sequences, but not for the mutated control sequences, which presumably represent nonspecific binding. Binding of GST-CHE to a sequence containing the TCP-binding site from the CCA1 promoter (Pruneda-Paz et al., 2009) was also measured and observed to lie within the low nanomolar range. We did attempt to assay other TCP family members but could not obtain protein of sufficiently high purity and concentration for use in these assays.

Prior work has shown that many macromolecular interactions are sensitive to temperature (Jarrett, 2000;

Schubert et al., 2003), whereas a defining feature of circadian rhythms is that they are temperature compensated (Pittendrigh, 1960). Intriguingly, the steady-state affinity of LHY, CCA1, and the LHY/CCA1 heterodimer for their cognate DNA sequences was observed to exhibit temperature compensation over a biologically relevant range ($Q_{10} < 1.3$). This is within the range of Q_{10} observed for circadian period over a range of organisms (Akman et al., 2008), including *Arabidopsis*.

Although we feel it to be unlikely that LHY and CCA1 binding, alone, constitutes the basis of temperature compensation in plants, it may make a relevant contribution—indeed it was not anticipated that the interaction between a recombinant transcription factor and a short stretch of double-stranded DNA in vitro might already exhibit such a feature. These data could provide another example of the hypothesized intramolecular temperature compensation (Ruoff et al., 2007), which has been observed for the auto-kinase/phosphatase activity of KaiC, a component of the cyanobacterial circadian clock (Tomita et al., 2005). In the case of LHY and CCA1, it is conceivable that as temperature increases, a reduction in the contribution of polar interactions to complex stability (from hydrogen bonds, salt bridges) is compensated by an increased contribution from hydrophobic interactions (solvent entropy effects, van der Waals), resulting in an interaction that is buffered against physiologically relevant temperature change.

Our observation raises the possibility that several clock components might possess an inherent capacity for temperature compensation (Dibner et al., 2009; Isojima et al., 2009; Mehra et al., 2009). The influence of individual, temperature-compensated biochemical processes on period will vary, however, as the period of a circadian rhythm in vivo is an emergent behavior of the underlying clock network. Mechanistic mathematical models can help to estimate the influence of each process, using the control coefficient for period (Ruoff et al., 2007; Akman et al., 2008). The equivalent experiment involves measuring the period of organisms where the relevant process is quantitatively altered (not abolished), at a range of temperatures, coupled with the extension of our in vitro measurement of parameter values to living cells.

It has been suggested previously that the densely packed nuclear environment limits the diffusive space available to macromolecules, resulting in their higher effective concentration and altering their kinetics in vivo (Grima and Schnell, 2008). Clock components will also be affected by the intracellular milieu, but it is unclear how typical the behavior of clock components is compared to other proteins. In keeping with this, in the presence of the branched polymer dextran, we observed a significantly higher apparent steady-state affinity of LHY for its cognate DNA sequence. This suggests that binding in vivo may be somewhat stronger than that determined outside a cellular context and that variation in crowding might affect regulation by LHY and CCA1. The in vitro parameter estimates reported here are starting points for refinement and comparison, which will be useful in constraining mathematical model development.

In parallel, it remains important to understand how the balance of temperature effects from the most significant clock components contributes to the emergent temperature response. Such effects include the multiple mechanisms affecting individual components, such as posttranslational modifications. It has previously been reported that CK2-mediated phosphorylation of CCA1 and by implication LHY has functional consequences for binding in vivo and in vitro (Daniel et al., 2004; Sugano et al., 1998; Sugano et al., 1999). Here, we have shown that phosphorylation of LHY in vitro results in a stronger steady-state affinity for its cognate DNA sequence. By mass spectrometric methods, we detected several phosphopeptides, some of which have been observed to be phospho-sites with functional relevance in LHY homologue CCA1. While it is likely that phosphorylation at distant sites in the molecule may have differential effects in vivo, the fact that a significant increase in steady-state affinity is observed upon in vitro phosphorylation, suggests that one role of CK2 modification may be to fine-tune DNA-protein interactions.

We anticipate that as more qualitative biochemical data describing different posttranslational aspects of clock components become available, this will facilitate the emergence of more accurate and detailed mathematical models of the cellular clock that will postulate clear and testable predictions of functional mechanisms.

ACKNOWLEDGMENTS

CSBE is a Centre for Integrative Systems Biology funded by BBSRC and EPSRC award D019621.

NOTE

Supplementary online material for this article is available on the *Journal of Biological Rhythms* Web site: http://jbr.sagepub.com/supplemental.

REFERENCES

Akman OE, Locke JC, Tang S, Carre I, Millar AJ, and Rand DA (2008) Isoform switching facilitates period control in the *Neurospora crassa* circadian clock. Mol Syst Biol 4:164.

Daniel X, Sugano S, and Tobin EM (2004) CK2 phosphorylation of CCA1 is necessary for its circadian oscillator function in Arabidopsis. Proc Natl Acad Sci U S A 101: 3292-3297.

Dibner C, Sage D, Unser M, Bauer C, d'Eysmond T, Naef F, and Schibler U (2009) Circadian gene expression is resilient to large fluctuations in overall transcription rates. EMBO J 28:123-134.

Edwards KD, Akman OE, Knox K, Lumsden PJ, Thomson AW, Brown PE, Pokhilko A, Kozma-Bognar L, Nagy F, Rand DA, et al (2010) Quantitative analysis of regulatory flexibility under changing environmental conditions. Mol Syst Biol 6:424.

Gould PD, Locke JCW, Larue C, Southern MM, Davis SJ, Hanano S, Moyle R, Milich R, Putterill J, Millar AJ, and Hall A (2006) The molecular basis of temperature compensation in the Arabidopsis circadian clock. Plant Cell 18:1177-1187.

Grima R and Schnell S (2008) Modelling reaction kinetics inside cells. Essays Biochem 45:41-56.

Harmer SL (2009) The circadian system in higher plants. Annu Rev Plant Biol 60:357-377.

Harmer SL and Kay SA (2005) Positive and negative factors confer phase-specific circadian regulation of transcription in Arabidopsis. Plant Cell 17:1926-1940.

Hofr C, Sultesova P, Zimmermann M, Mozgova I, Prochazkova Schrumpfova P, Wimmerova M, and Fajkus J (2009) Single-myb histone proteins from *Arabidopsis thaliana*: quantitative study of telomere binding specificity and kinetics. Biochem J 419:221-228.

Isojima Y, Nakajima M, Ukai H, Fujishima H, Yamada RG, Masumoto KH, Kiuchi R, Ishida M, Ukai-Tadenuma M, Minami Y, et al. (2009) CKIepsilon/delta-dependent phosphorylation is a temperature-insensitive, period-determining process in the mammalian circadian clock. Proc Natl Acad Sci U S A 106:15744-15749.

Jarrett HW (2000) Temperature dependence of DNA affinity chromatography of transcription factors. Anal Biochem 279:209-217.

Locke JC, Kozma-Bognar L, Gould PD, Feher B, Kevei E, Nagy F, Turner MS, Hall A, and Millar AJ (2006) Experimental validation of a predicted feedback loop in the multi-oscillator clock of *Arabidopsis thaliana*. *Mol Syst Biol* 2:59.

Locke JC, Southern MM, Kozma-Bognar L, Hibberd V, Brown PE, Turner MS, and Millar AJ (2005) Extension of a genetic network model by iterative experimentation and mathematical analysis. Mol Syst Biol 1:2005.0013.

Lu SX, Knowles SM, Andronis C, Ong MS, and Tobin EM (2009) CIRCADIAN CLOCK ASSOCIATED1 and LATE ELONGATED HYPOCOTYL function synergistically in the circadian clock of Arabidopsis. Plant Physiol 150: 834-843.

Majka J and Speck C (2007) Analysis of protein-DNA interactions using surface plasmon resonance. Adv Biochem Eng Biotechnol 104:13-36.

McClung CR (2006) Plant circadian rhythms. Plant Cell 18: 792-803.

Mehra A, Shi M, Baker CL, Colot HV, Loros JJ, and Dunlap JC (2009) A role for casein kinase 2 in the mechanism underlying circadian temperature compensation. Cell 137:749-760.

Mouillon JM, Eriksson SK, and Harryson P (2008) Mimicking the plant cell interior under water stress by macromolecular crowding: disordered dehydrin proteins are highly resistant to structural collapse. Plant Physiol 148:1925-1937.

Oda M, Furukawa K, Sarai A, and Nakamura H (1999) Kinetic analysis of DNA binding by the c-Myb DNA-binding domain using surface plasmon resonance. FEBS Lett 454:288-292.

Persson S (2008) Calibration free analysis to measure the concentration of active proteins. Biosci Technol 32:14-18.

Pittendrigh CS (1960) Circadian rhythms and the circadian organization of living systems. Cold Spring Harb Symp Quant Biol 25:159-184.

Pokhilko A, Hodge SK, Stratford K, Knox K, Edwards KD, Thomson AW, Mizuno T, and Millar AJ (2010) Data assimilation constrains new connections and components in a complex, eukaryotic circadian clock model. Mol Syst Biol 6:416.

Pruneda-Paz JL, Breton G, Para A, and Kay SA (2009) A functional genomics approach reveals CHE as a component of the Arabidopsis circadian clock. Science 323:1481-1485.

Richter K, Nessling M, and Lichter P (2008) Macromolecular crowding and its potential impact on nuclear function. Biochim Biophys Acta 1783:2100-2107.

Ruoff P, Zakhartsev M, and Westerhoff HV (2007) Temperature compensation through systems biology. FEBS J 274:940-950.

Schubert F, Zettl H, Hafner W, Krauss G, and Krausch G (2003) Comparative thermodynamic analysis of DNA-protein interactions using surface plasmon resonance and fluorescence correlation spectroscopy. Biochemistry 42:10288-10294.

Sugano S, Andronis C, Green RM, Wang ZY, and Tobin EM (1998) Protein kinase CK2 interacts with and phosphorylates the Arabidopsis circadian clock-associated 1 protein. Proc Natl Acad Sci U S A 95:11020-11025.

Sugano S, Andronis C, Ong MS, Green RM, and Tobin EM (1999) The protein kinase CK2 is involved in regulation of circadian rhythms in Arabidopsis. Proc Natl Acad Sci U S A 96:12362-12366.

Tomita J, Nakajima M, Kondo T, and Iwasaki H (2005) No transcription-translation feedback in circadian rhythm of KaiC phosphorylation. Science 307:251-254.

Yakir E, Hilman D, Kron I, Hassidim M, Melamed-Book N, and Green RM (2009) Posttranslational regulation of CIRCADIAN CLOCK ASSOCIATED1 in the circadian oscillator of Arabidopsis. Plant Physiol 150:844-857.

Zeilinger MN, Farre EM, Taylor SR, Kay SA, and Doyle FJ, 3rd (2006) A novel computational model of the circadian clock in Arabidopsis that incorporates PRR7 and PRR9. Mol Syst Biol 2:58.

Supplementary Online Material

Circadian Clock Parameter Measurement: Characterisation of Clock Transcription Factors using Surface Plasmon Resonance.

John S. O'Neill, Gerben van Ooijen, Thierry Le Bihan and Andrew J. Millar

MATERIALS AND METHODS

Mass Spectrometry

Materials: Acetonitrile and water used for LC/MS/MS analysis or sample preparation were of HPLC quality (Fisher, UK). Formic acid was Suprapure 98-100%, (Merck, Darmstadt, Germany) and trifluoroacetic acid 99% purity sequencing grade (Fisher, UK). All other chemicals used in the preparation of sample were of reagent grade or better (Sigma, UK), unless specified. Sequencing grade modified porcine trypsin was purchased from Promega (UK). All connector fittings were from Upchurch Scientific (Hichrom and Restek, UK).

Sample preparation: Sample estimated to 500 nM in 0.04% P20, 20 mM Hepes 150 mM NaCl and 1 mM TCEP was digested in-solution as followed: The sample was made up to 850 μl water plus 300 μl 8M urea, reduced with 100 μl DTT 200mM for 30min at RT, alkylated with 200 μl iodoacetaminde 500 mM and trypsinized with 50 μg of trypsin.

The sample was cleaned on SPE using C18 Sep-Pak (Water, UK), the eluate was dry under low pressure and reconstituted in 50 µL of 0.1% (v/v) formic acid 2.5 % acetonitrile (solution 1) and 50 µL 80% acetonitrille 0.1% TFA 200 mg/ml of 2,5-dihydroxy-benzoic acid (solution 2).

*Phosphopeptide enrichment on a titanium column***:** Phosphopeptide enrichment method used is close to the method presented by Thingholm *et al.*, 2006 except for the format of the column and solution volume. Handmade titanium columns (Titansphere 10 µm media) packed into a 4 cm x 400 µm column made from 1/16 peek tubing and external frits from Upchurch scientific were operated with an handmade pressure vessel.

Prior to use, the columns were conditioned with 200 µl 80% acetonitrille 0.1% TFA (solution 3). Samples were loaded at approx 3-5 µl/min. The column was washed with 50ul solution 1 followed by 50 µl solution 3 and non specific interaction were reduce with an additional wash with 200ul solution 2 followed by a wash with 400 µl solution 3. Phosphopeptide elution was done in a 3 steps manner: first elution was done with a 30ul ammonia pH 10 (approx 250 µl ammonium hydroxide 7 N into 25 mL: solution 4), quickly a second elution was performed with 40 µl solution 4 plus 10 µl 7 N ammonium hydroxide and a third elution was performed with 40ul acetonitrille plus 10 ul 7 N ammonium hydroxide. The 3 eluates were combined, dry under low pressure and reconstitute in 30 µl of water:acetonitrile (97.5:2.5) and formic acid 0.1%, spin at 14 000 rpm for 5 min and 8 µl of the sample was injected on LC-MS

*HPLC and Mass Spectrometry***:** Micro-HPLC-MS/MS analysis were performed using an on-line system consisting of a micro-pump Agilent 1200 binary HPLC system (Palo Alto, CA) coupled

to an hybrid LTQ-Orbitrap XL instrument (ThermoQuest Corp, San Jose, CA). The LTQ-Orbitrap-XL was controlled through Xcalibur 2.0.7 and LTQ Orbitrap XL MS2.4SPI. All the LC-MS conditions were similar to the one previously described in Luke-Glaser *et al.*, 2007. In data dependant mode, the MS acquisition settings were as follows: a single FT scan at a resolution of 60k in profile mode (400-2000 m/z) was first performed with no lock mass function followed by 3 data dependent MS/MS scans of the 3 most intense ions in LTQ centroid mode with a mass window of 3amu.

In MS3 targeted mode: A series of few experiments were done in a more targeted mode where specific MS3 were acquired on few selected MS2 fragment associated to specific daughter ions in order to increase confidence in some of the phosphopeptides detected.

*Data Processing***.** Mascot Generic Format (MGF) input files were generated with the EXTRACT_MSN tool (Bioworks 3.3, ThermoQuest Corp, San Jose, CA MS/MS data were searched using MASCOT Version 2.2 (Matrix Science Ltd, UK) against a Esherishia coli database (14588 sequences March 2008) downloaded from NCBI including the construct MBP-AtLHY .

All Mascot searches were performed using a maximum missed-cut value of 1, mass modifications are those found at www.unimod.org as described before in Luke-Glaser *et al.*, 2007. Each Mascot peptides identification were manually verified, other fragmentation possibility were checked using Protein Prospector (http://prospector.ucsf.edu) mostly b and y ion both in their phosphorylated form as well as their phosphate lost form. Other minor fragmentation possibility such as multiple losses and internal fragment were also looked at. We

verify that all major intense transitions can be explained by the lost of the phosphate moiety in the form of H_3PO_4 and or HPO_3..

Supplementary References:

Thingholm TE, Jørgensen TJ, Jensen ON, Larsen MR.
Highly selective enrichment of phosphorylated peptides using titanium dioxide
Nat Protoc. 2006;1(4):1929-35

Luke-Glaser S, Roy M, Larsen B, Le Bihan T, Metalnikov P, Tyers M, Peter M, Pintard L. CIF-1, a shared subunit of the COP9/signalosome and eukaryotic initiation factor 3 complexes, regulates MEL-26 levels in the Caenorhabditis elegans embryo. Mol Cell Biol. 2007 Jun;27(12):4526-40.

O'Neill *et al*, Supplementary Figure 1

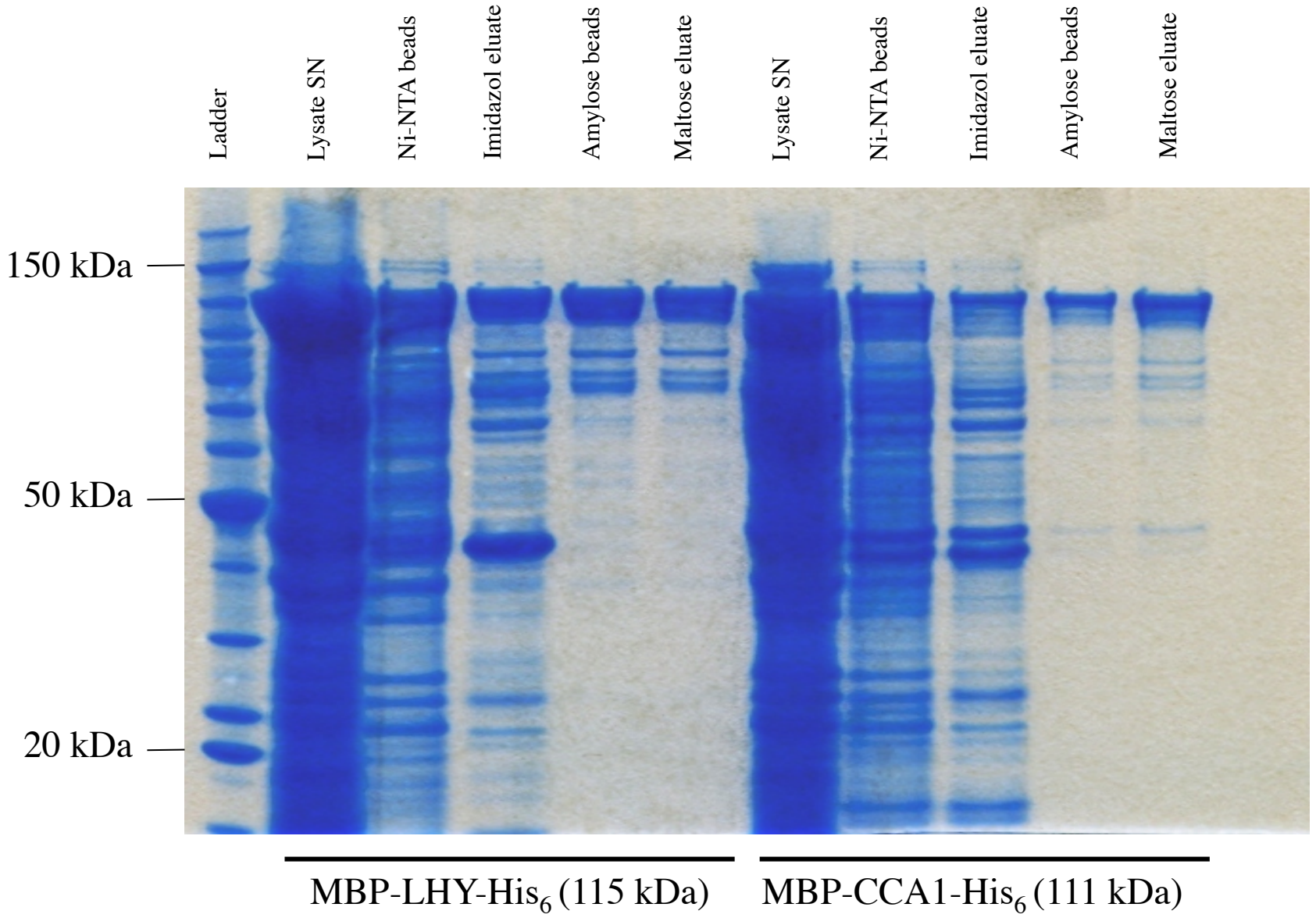

Supplementary Figure 1. Representative coomassie-stained gel showing dual tag affinity purification of LHY and CCA1.

A

E S Q V G N I N N Q s D E K

Precursor ion 821.3401amu; Δmass -1.38ppm; score 35

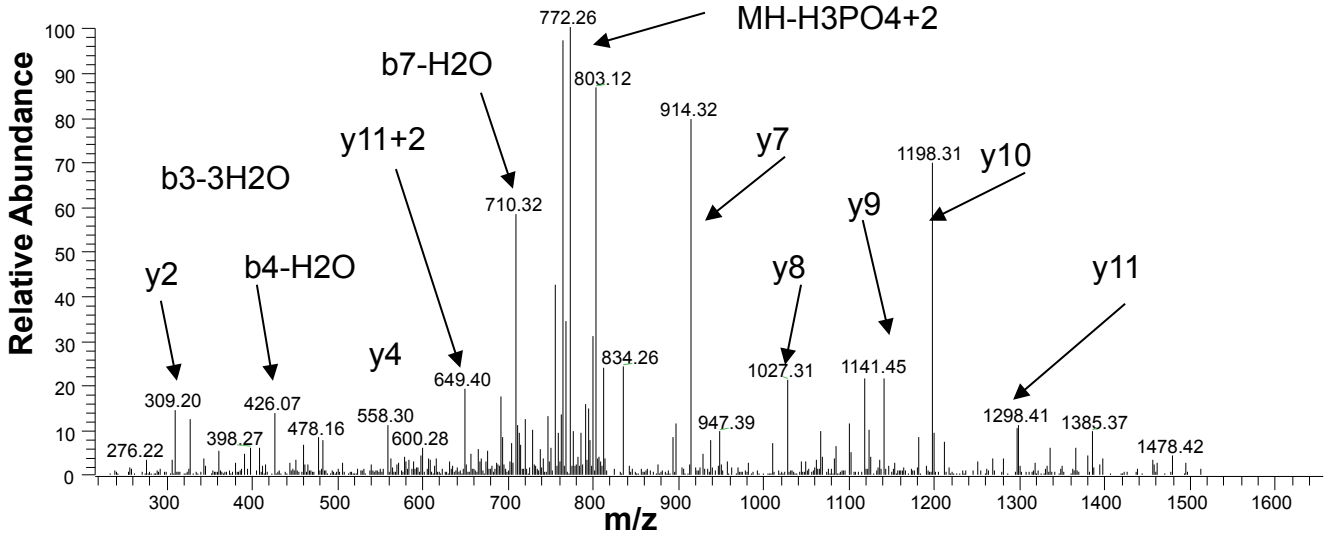

MS^3: y7 914.32 amu

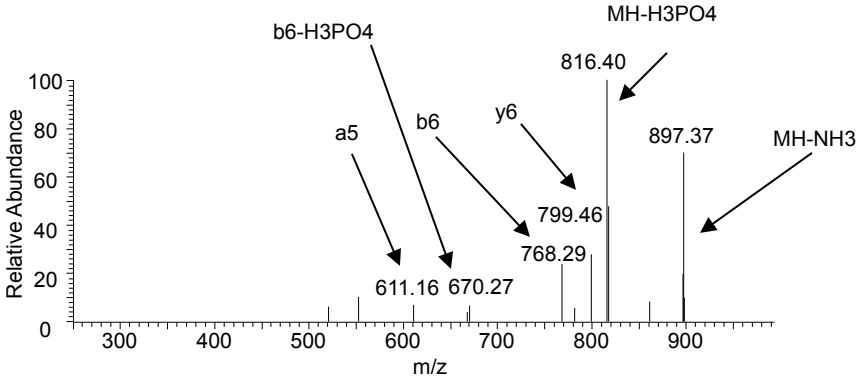

B

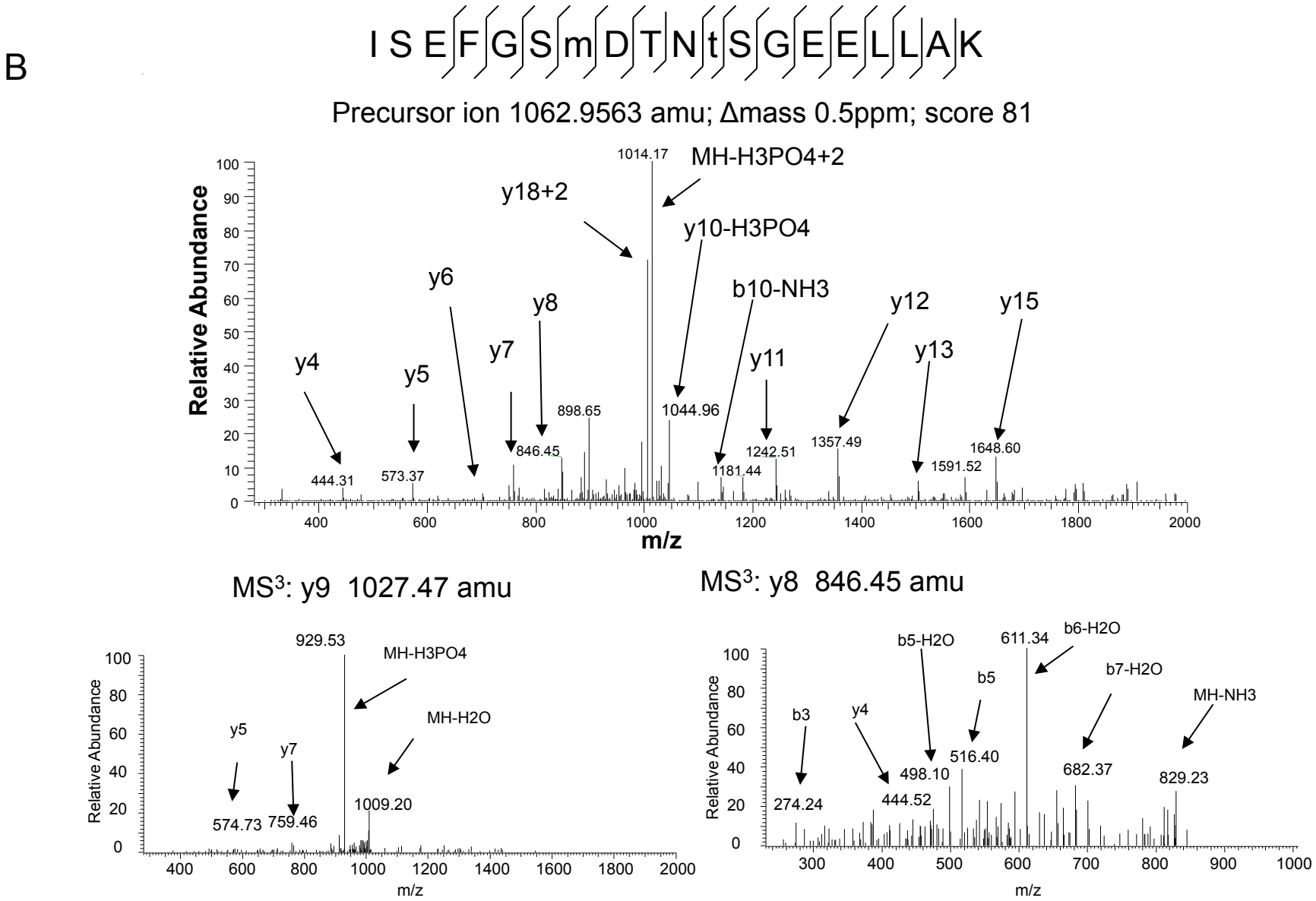
I S E F G S m D T N t S G E E L L A K
Precursor ion 1062.9563 amu; Δmass 0.5ppm; score 81
Relative Abundance
m/z
1014.17
MH-H3PO4+2
y18+2
y10-H3PO4
y6
b10-NH3
y8
y12
y15
y4
y5
y7
y11
y13
898.65
1044.96
846.45
1242.51
1357.49
1648.60
444.31
573.37
1181.44
1591.52
MS3: y9 1027.47 amu
929.53
MH-H3PO4
MH-H2O
y5
y7
1009.20
574.73
759.46
MS3: y8 846.45 amu
b5-H2O
611.34
b6-H2O
b7-H2O
b5
MH-NH3
b3
y4
516.40
498.10
682.37
829.23
274.24
444.52

C

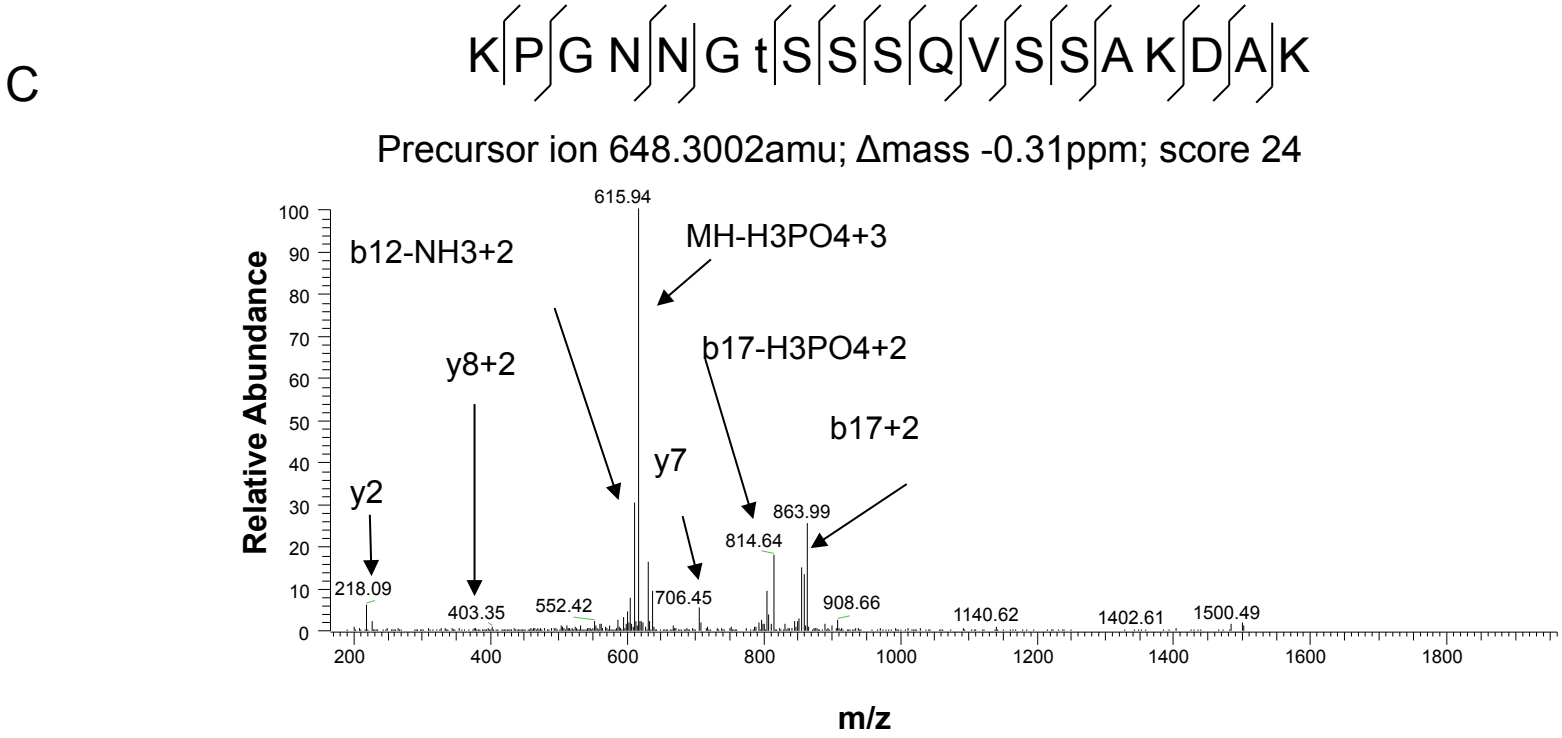
K P G N N G t S S S Q V S S A K D A K
Precursor ion 648.3002amu; Δmass -0.31ppm; score 24
Relative Abundance
m/z
615.94
MH-H3PO4+3
b12-NH3+2
y8+2
b17-H3PO4+2
b17+2
y7
y2
863.99
814.64
218.09
403.35
552.42
706.45
908.66
1140.62
1402.61
1500.49

D

Q N T A L Q D Q N L A S K S P A S s S D D S D E T G V T K

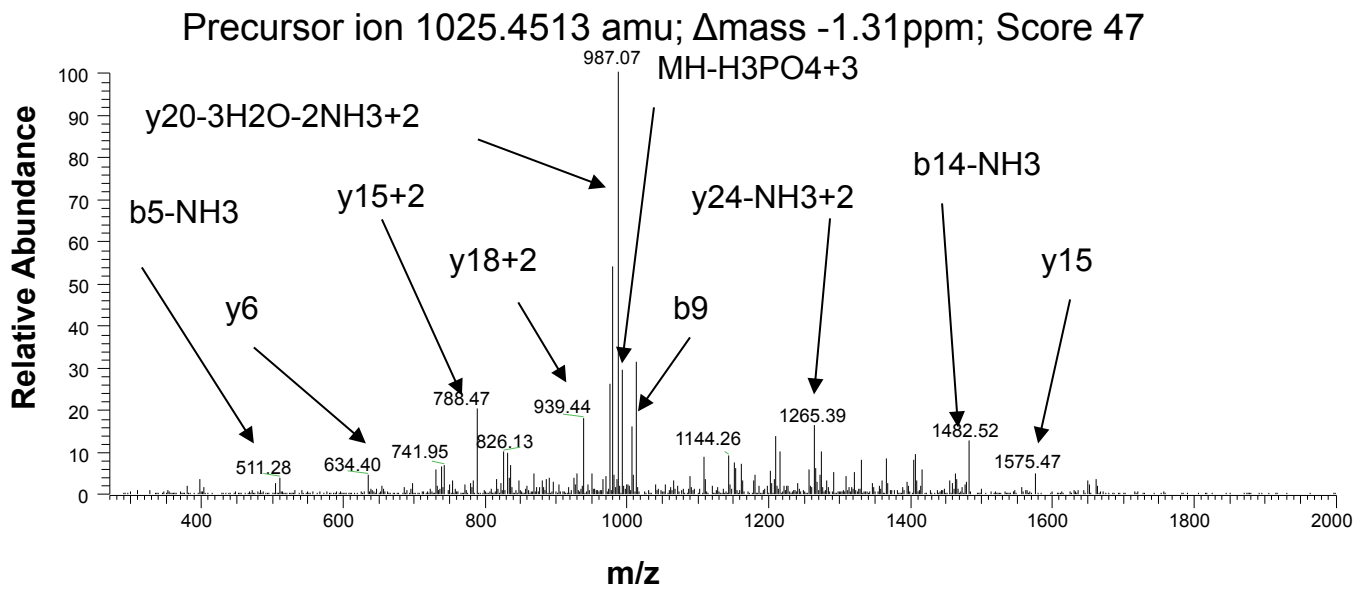

MS^3: y23+2 1210.01 amu

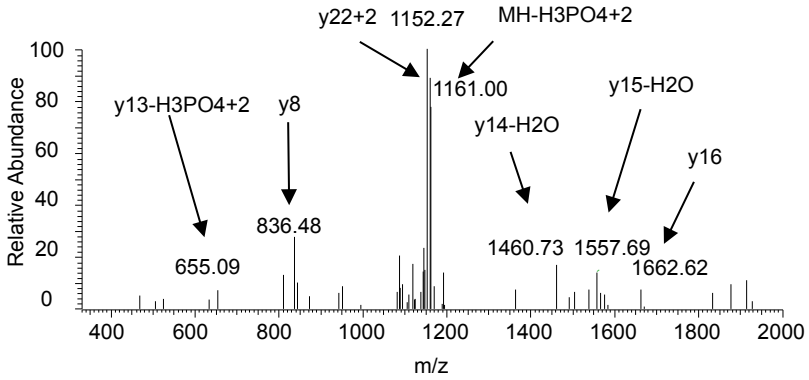

MS^3: y15+2 788.47 amu

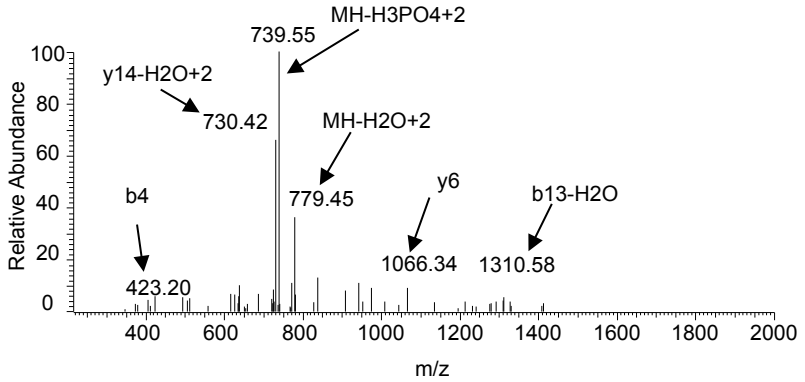

E

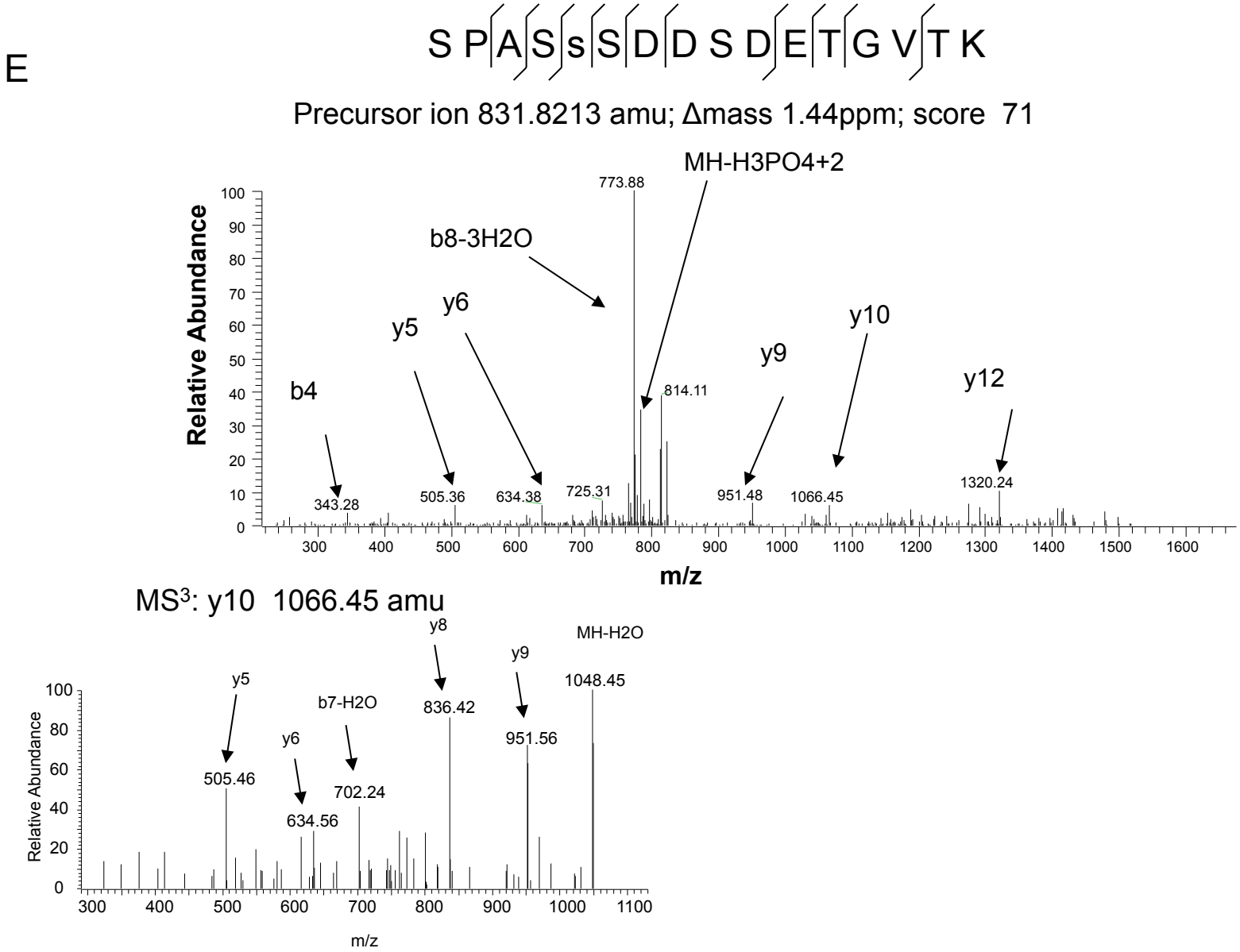
S P A S s S D D S D E T G V T K
Precursor ion 831.8213 amu; Δmass 1.44ppm; score 71
MH-H3PO4+2
773.88
b8-3H2O
y6
y5
y10
y9
y12
b4
814.11
343.28
505.36
634.38
725.31
951.48
1066.45
1320.24
Relative Abundance
m/z
MS3: y10 1066.45 amu
y8
MH-H2O
y9
y5
1048.45
b7-H2O
836.42
y6
951.56
505.46
702.24
634.56
Relative Abundance
m/z

F

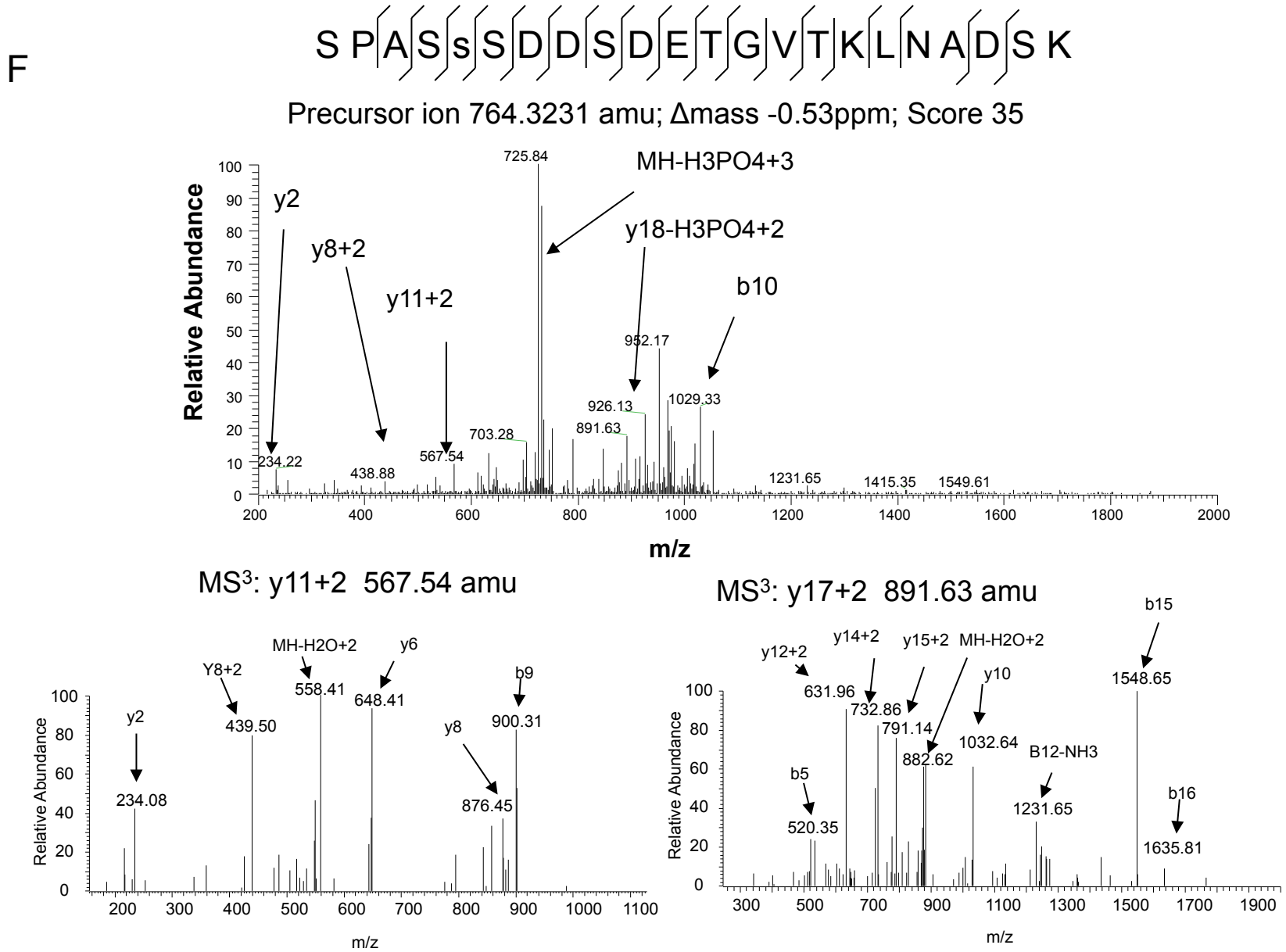
S P A S s S D D S D E T G V T K L N A D S K
Precursor ion 764.3231 amu; Δmass -0.53ppm; Score 35
Relative Abundance
m/z
y2
y8+2
y11+2
MH-H3PO4+3
y18-H3PO4+2
b10
725.84
952.17
926.13
1029.33
891.63
703.28
567.54
234.22
438.88
1231.65
1415.35
1549.61
MS3: y11+2 567.54 amu
y2
Y8+2
MH-H2O+2
y6
b9
y8
234.08
439.50
558.41
648.41
900.31
876.45
MS3: y17+2 891.63 amu
y12+2
y14+2
y15+2
MH-H2O+2
y10
b15
b5
B12-NH3
b16
631.96
732.86
791.14
882.62
1032.64
1231.65
520.35
1548.65
1635.81

G

S S C G S N T P S G s D A E t D A L D K

Precursor ion 1079.8783 amu; Δmass -1.21ppm; score 80

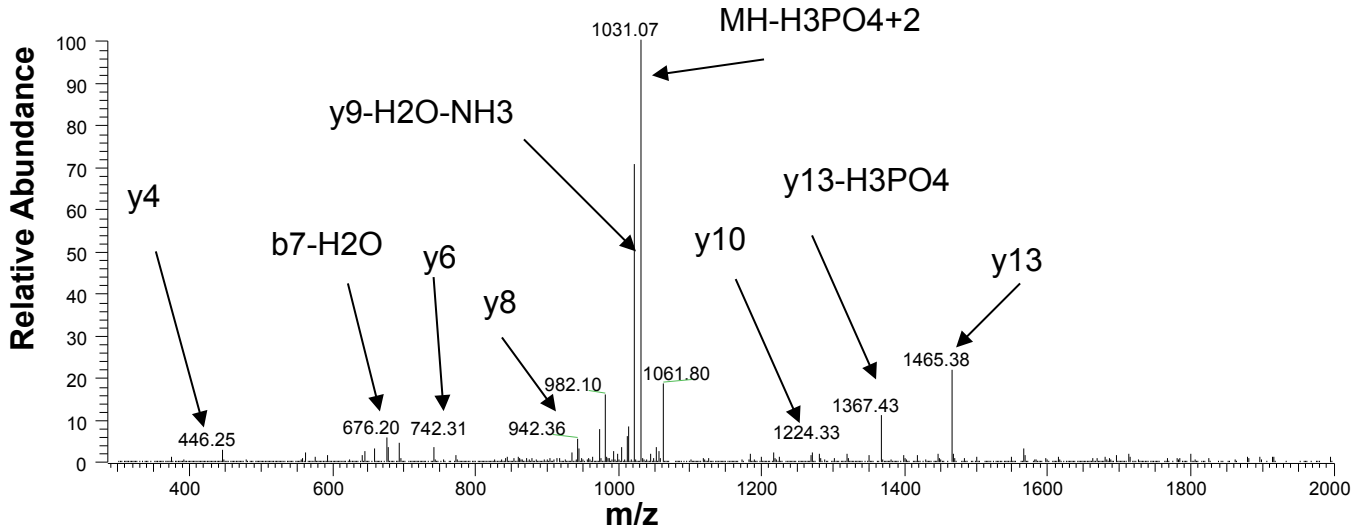

MS^3: y10 1224.33 amu

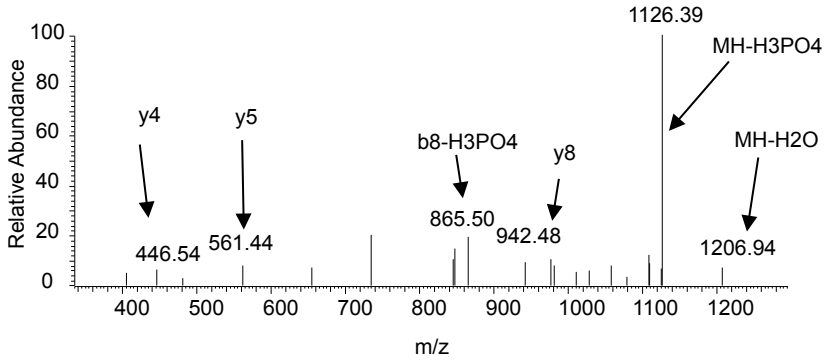

MS^3: y6 742.31 amu

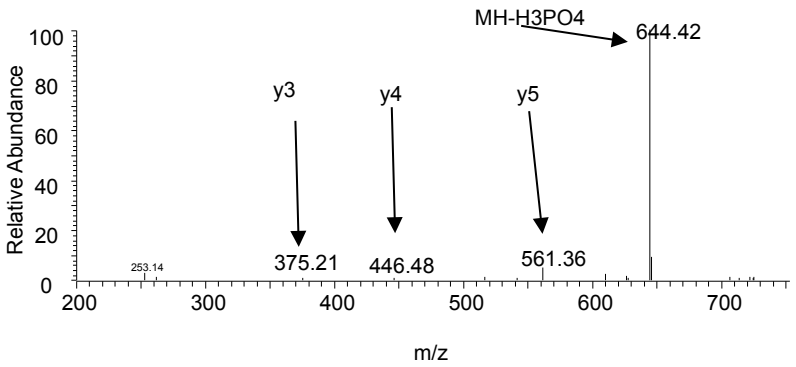

H

S S C G S N T P s G s D A E t D A L D K

Precursor ion 1119.8614 amu; Δmass -1.18ppm; score 68

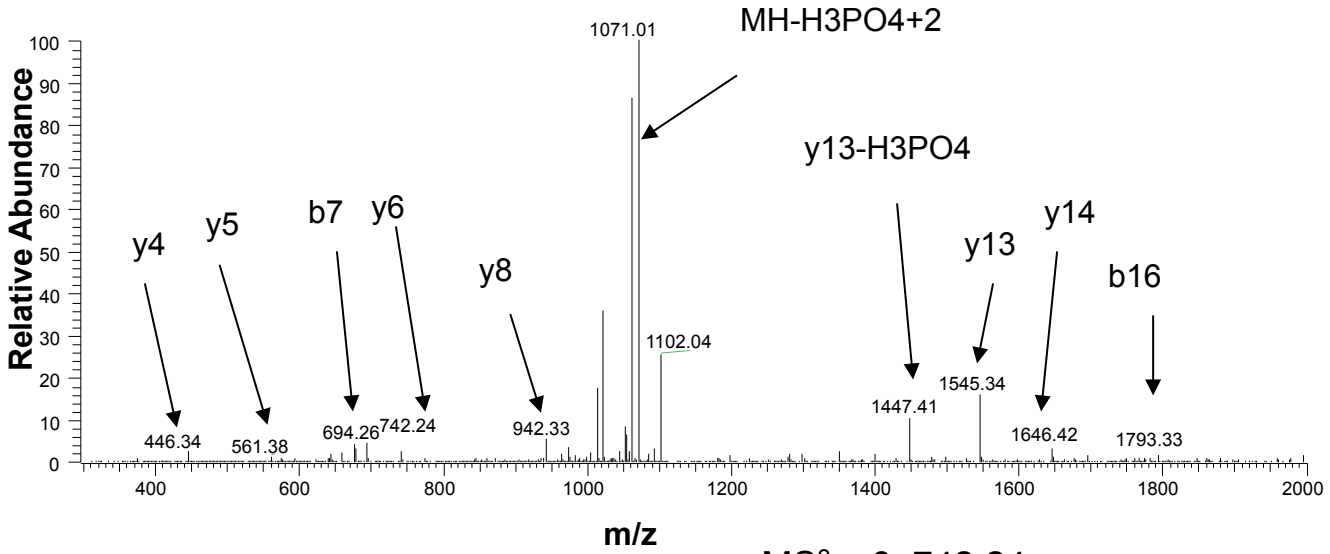

MS^3: y6 742.24 amu

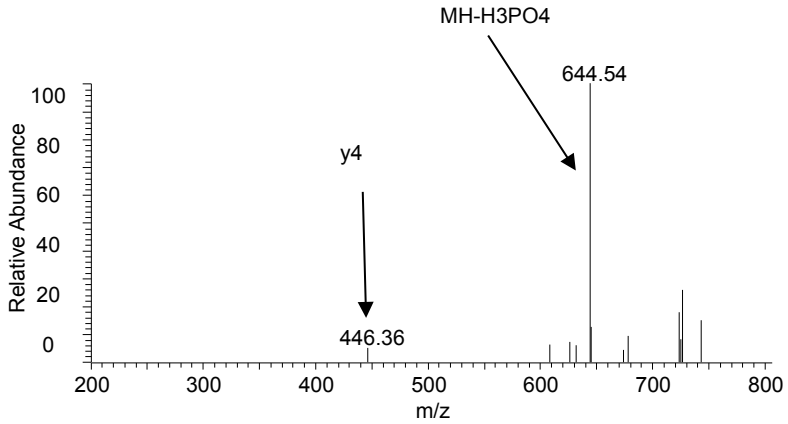

I

S S C G S N T P S G s D A E T D A L D K

Precursor ion 1039.8966 amu; Δmass 0.16ppm; score 94

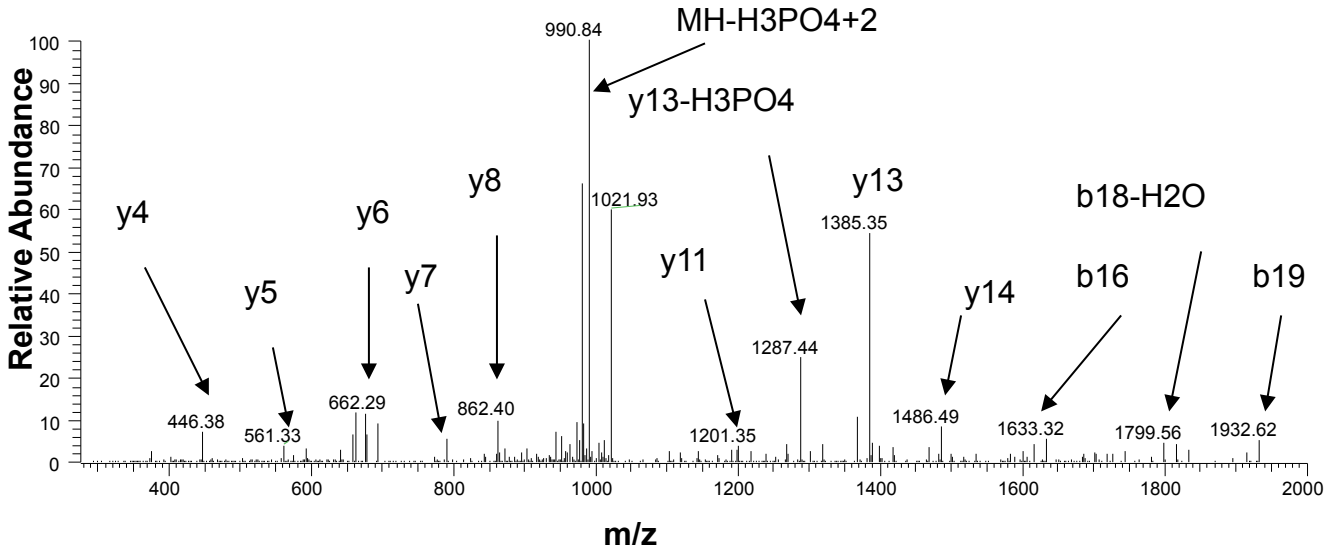

MS³: y8 862.40 amu

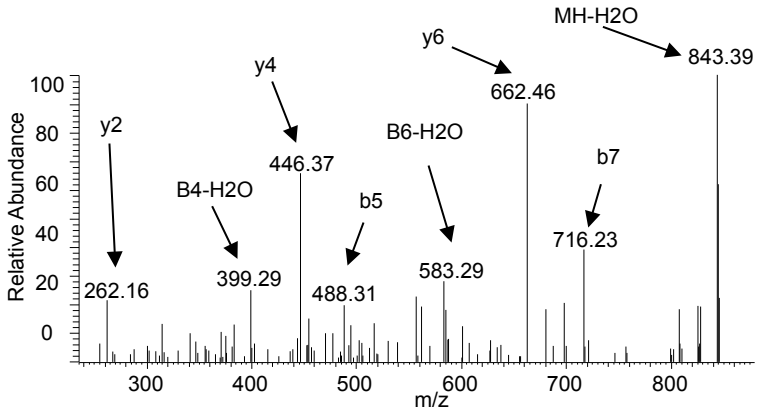

MS³: y13 1385.54 amu

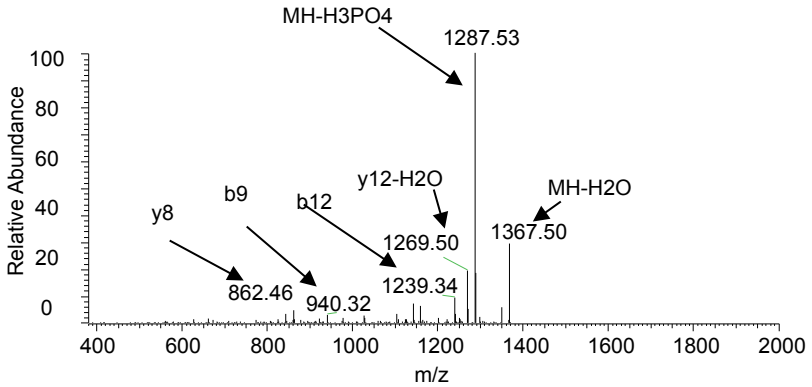

J

S S C G S N T P s G S D A E T D A L D K m E K

Precursor ion 1241.9821 amu; Δmass -0.69ppm; score 59

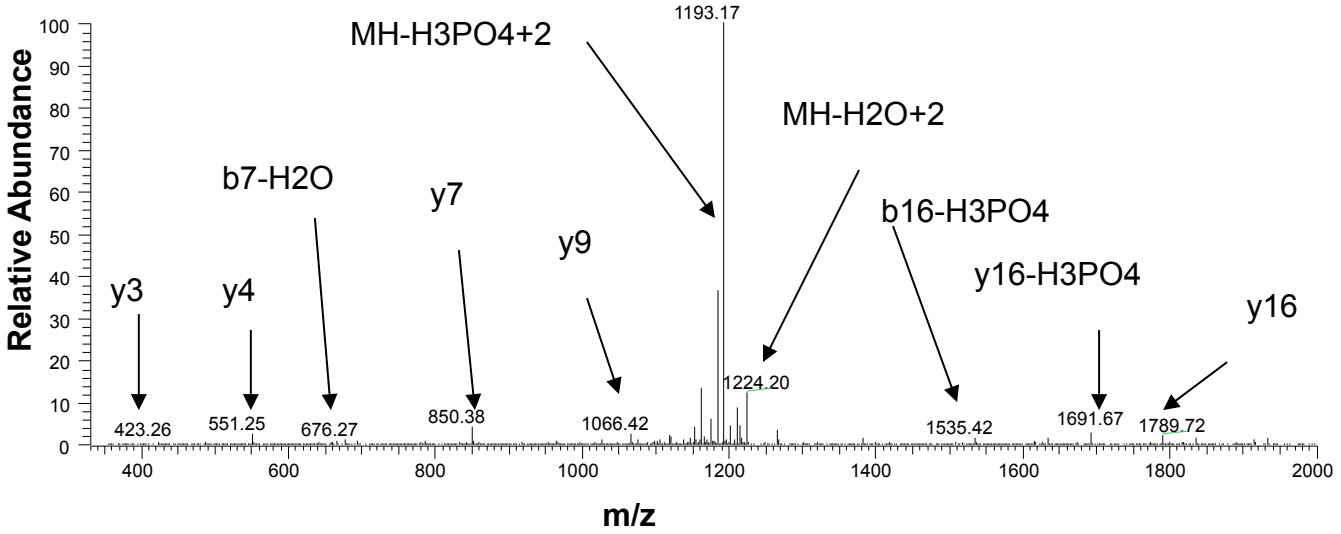

MS^3: y9 1066.42 amu

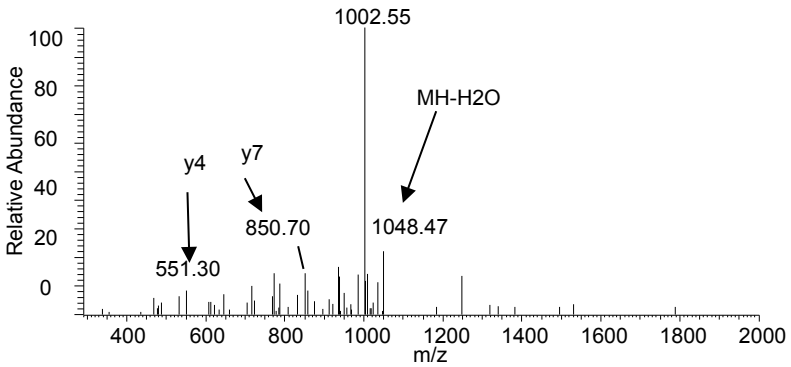

MS^3: y16 1789.72 amu

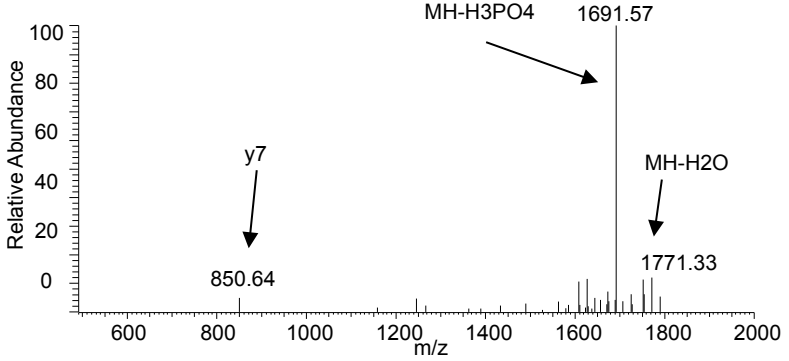

K

S S C G S N T P S G s D A E T D A L D K M E K

Precursor ion 828.3243 amu; Δmass -0.11ppm; score 38

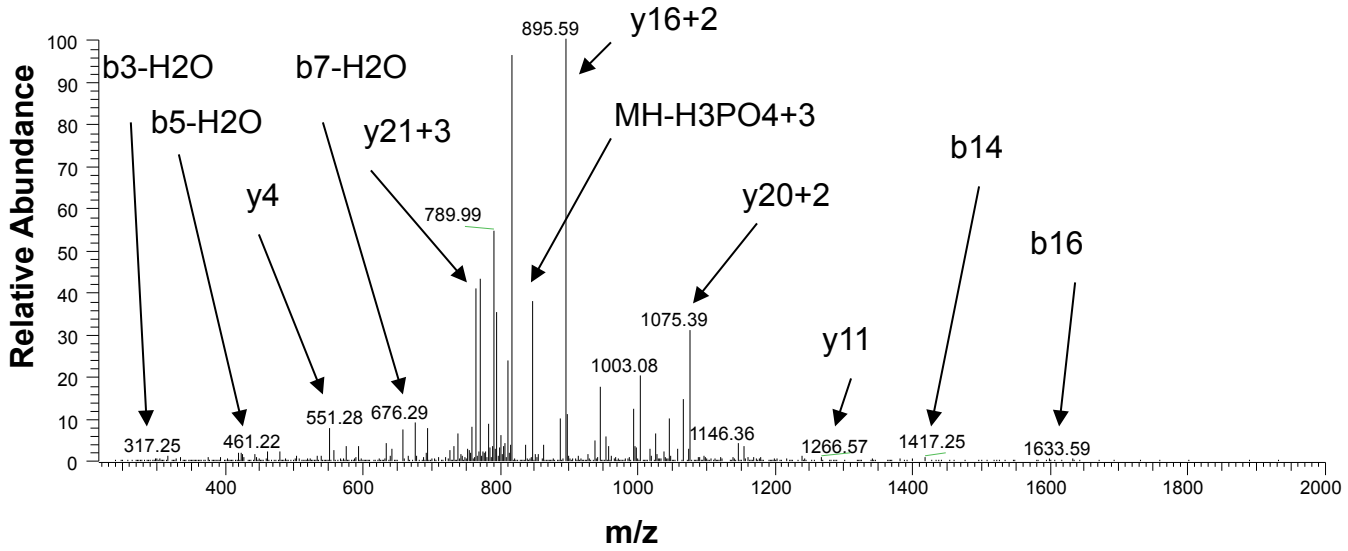

MS^3: y16+2 895.59 amu

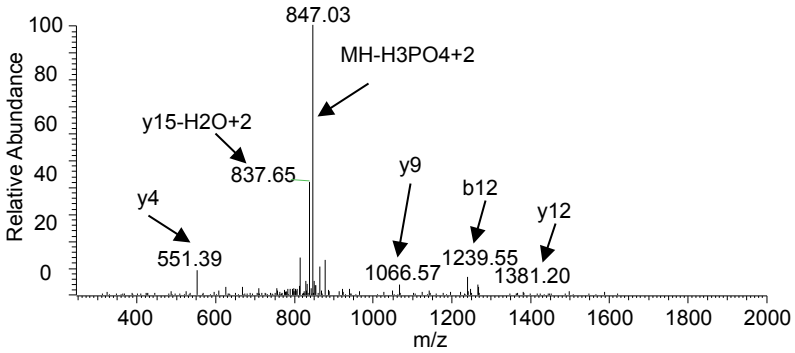

MS^3: y11 1266.57 amu

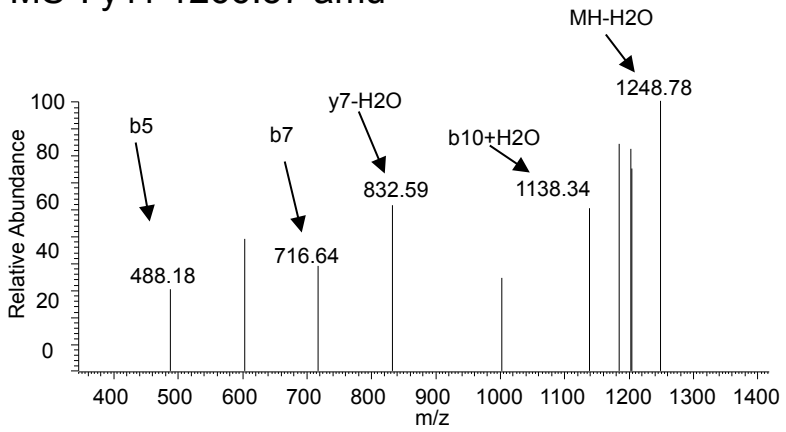

L

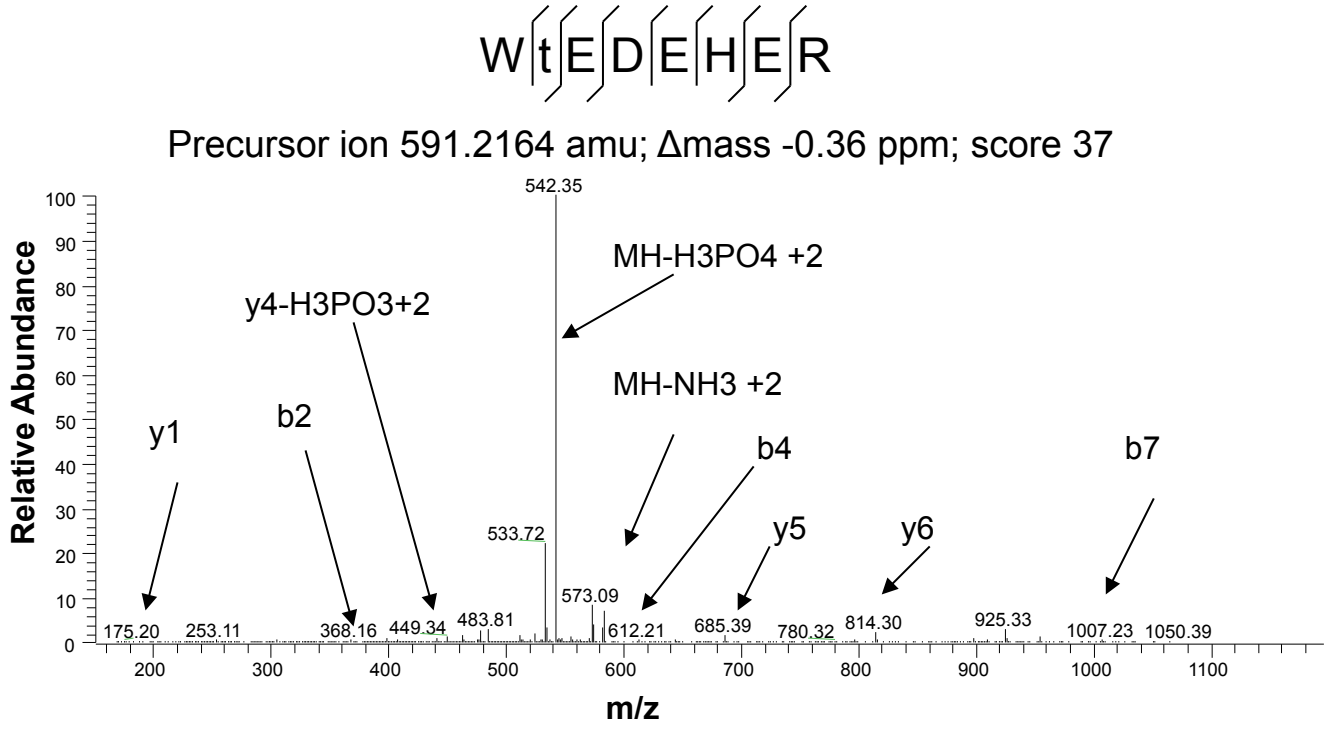

M

m/z	z	error (Da)	misscut	Score	Expect	Sequence	Modification	Phosphorylation site	in CCA1	Notes
821.3401	2	-0.0023	0	35.13	0.0014	(K)ESQVGNINNQSDEK(V)	Phospho (ST)	S628		see note 1
1062.9563	2	0.0011	0	81.02	7.50E-08	(R)ISEFGSMDTNTSGEELLAK(A)	Oxidation (M); Phospho (ST)	T5	yes	
648.3002	3	-0.0006	1	24.25	0.032	(R)KPGNNGTSSSQVSSAKDAK(L)	Phospho (ST)	T113		
1025.4513	3	-0.004	1	46.94	0.00029	(K)QNTALQDQNLASKSPASSSDDSDETGVTK(L)	Phospho (ST)	S419		
831.8213	2	-0.0024	0	71.49	3.70E-07	(K)SPASSSDDSDETGVTK(L)	Phospho (ST)	S419		
764.3231	3	-0.0012	1	34.61	0.0025	(K)SPASSSDDSDETGVTKLNADSK(T)	Phospho (ST)	S419		
1079.8783	2	-0.0026	0	79.55	2.30E-08	(R)SSCGSNTPSGSDAETDALDK(M)	2 Phospho (ST)	S476 + T480		
1119.8614	2	-0.0026	0	68.25	1.50E-07	(R)SSCGSNTPSGSDAETDALDK(M)	3 Phospho (ST)	S474 + S476 + T481		
1039.8966	2	0.0003	0	93.59	1.70E-09	(R)SSCGSNTPSGSDAETDALDK(M)	Phospho (ST)	S476	yes	
1241.9821	2	-0.0017	1	59.46	6.90E-06	(R)SSCGSNTPSGSDAETDALDKMEK(D)	Oxidation (M); Phospho (ST)	S474	yes	
828.3243	3	-0.0003	1	38.21	0.00092	(R)SSCGSNTPSGSDAETDALDKMEK(D)	Oxidation (M); Phospho (ST)	S476	yes	
591.2164	2	-0.0004	0	36.9	0.00027	(R)WTEDEHER(F)	Phospho (ST)	T28		

note 1: The most probable assignment predicted by Mascot is with the serine phosphorylated in S619 which does not explain y7, y8, y9, y10 and y11. We therefore chose the second most probable hit, also confirmed by MS3 on y7.

Supplementary Figure 2. Identification of *in vitro* phospho-sites in recombinant LHY.
A-L) Selected CID MS2 and MS3 of the fragmentation pattern of the phosphopeptides detailed in table M. Only significant fragment ions have been labeled. MS3 are shown when ambiguous phospho-site assignments are detected however for (c), MS3 signal was too low.
M) Table of the detected phosphopeptides by micro-LC-MS after on-column TiO_2 enrichment. 9 unique phospho-sites were identified, as well as 2 multiply phosphorylated peptides.